Korean J. Chem. Eng., 36(6), 996-1003 (2019)
DOI: 10.1007/s11814-019-0276-0

pISSN: 0256-1115
eISSN: 1975-7220

Development of a low environmental impact, porous solar absorber coating utilizing binary/ternary solvent blends for CSP systems

John Miller*,‡, Kathy Nwe*,‡, Yongjoon Youn*,‡, Kyungjun Hwang*, Chulmin Choi*, Paul Waliaula Mola II*, Youngjin Kim*,†, and Sungho Jin*,,†**

*NanoSD, Inc, 11575 Sorrento Valley Rd, Suite 200, San Diego, CA 92121, United States
**Department of Mechanical & Aerospace Engineering, University of California San Diego, 9500 Gilman Dr., La Jolla, CA 92093, United States
(*Received 16 February 2019 • accepted 16 April 2019*)

Abstract−Concentrated solar power utilizes a field of mirrors to redirect solar rays onto a central receiver to generate thermal energy through heat transfer media and a Rankine steam cycle. To effectively transfer heat to the heat transfer material, the receiver has to efficiently convert/absorb the incoming solar flux without losing energy to radiation. Receivers are coated with a solar absorber coating evaluated with a figure of merit which weighs the energy absorbed by the sample against the total incident energy. The structure of the painted coating plays a large part in the long-term stability and optical properties of the solar absorber coatings. We investigated the effects of different solvents on the micro-structure of black oxide coated paint tiles and evaluated the stability of the paint colloid using the Gibbs free energy of mixing. We also investigated the use of low environmental impact solvents as potential alternates to standard solvents to create low-stress films. The results show that paint blends thinned by blends of dimethyl carbonate and tert-butylbenzene have low-stress surface morphology with pore-like structures due to the favorable Gibbs free energy value of the colloid and reduced evaporation rate of the primary solvents. These coatings also exhibited strong optical performance with figure of merit and solar absorbance values of 91.60% and 96.86%, making them ideal coatings for next generation concentrated solar power plants.

Keywords: Concentrated Solar Power, Black Paint, Binary/Ternary Solvent, Porous Paint

INTRODUCTION

Solar energy is a growing source of renewable energy which can compete with fossil fuels and nuclear energy, the leading sources of energy generation today. The two most prominent forms of solar energy generation are photovoltaic (PV) solar cells and concentrated solar power (CSP) plants. PV solar cells use the photoelectric effect to generate electricity, where the PV solar cell absorbs incident light, which causes the emission of a photon. The emission causes charge carriers to move in the PV material generating a current, which in turn generates electricity [1,2]. On the other hand, CSP uses an array of mirrors to reflect and concentrate light onto a central receiver. This receiver has a heat exchange fluid running through it, which heats up when light waves are focused on it. The heat exchange fluid runs counter to a water stream, vaporizing the water in a steam turbine to generate mechanical work, and converting that work into electricity [3,4].

One of the benefits of the CSP Plants over PV solar fields is the ability to generate power even when there is no solar irradiance. CSP towers can store excess molten salt generated during the day and use it at night when there is no solar irradiance [5]. This dramatically helps bring down the levelized cost of electricity (LCOE). Another way to bring down the LCOE is to increase the heat transfer ability of the central receiver at temperatures up to 800 °C [6]. This can be accomplished by optimizing a receiver coating with high solar absorptivity in the UV-Vis-NIR range and low thermal emissivity in the IR-range. The current industry coating for CSP receivers is Pyromark 2500 (Tempil Inc, Ltd., USA). Nevertheless, according to Sandia National Labs, Pyromark Paint has low thermal stability at the higher operating temperatures of next generation CSP Paints [7]. Therefore, an alternative is required with high-temperature stability at 800 °C and enhanced optical properties.

Spinel ceramic black oxide pigments, such as $CuCr_2O_4$ and $CuCrMnO_4$, have been shown to have strong light-absorbing properties in the UV-Vis and NIR spectrum [8,9]. The spinel crystal structure also has high-temperature degradation resistance, making it perfectly suitable for the high operating temperature of future CSP plants [10,11]. Mixing these pigments with high-temperature silicone resins can make excellent coatings for long-lasting high-temperature black coatings [8]. Even with these high performing materials, it is still highly desirable to control the surface morphology and structure for further enhanced coating capabilities.

Light-trapping nanostructures offer a coating solution for central receivers that can significantly increase the performance of a coating. There are several types when developing a solar absorbing coating: 1) intrinsic absorbers, 2) semiconductor-metal tandems, 3) multilayer absorbers, 4) metal-dielectric composite, 5) surface texturing and 6) solar-transmitting coating/blackbody-like absorber [12]. All have their own advantages and disadvantages but experi-

†To whom correspondence should be addressed.
E-mail: narashia@gmail.com, jin1234jin@gmail.com
‡These authors contributed equally to this work.

ence difficulties during commercialization. Another method of introducing light trapping nanostructures into the film is with sacrificial polymers dispersed in the paint matrix [8]. After high-temperature annealing, the polymer beads decompose, leaving behind an empty pore in its place. Using these pores not only helps with the optical performance of the paint but also provides some mechanical relief, represented by reduced surface cracking [13]. However, manufacturing costs of coatings using these beads are extravagant due to the high capital cost of the beads and the additional stages required for paint processing for dispersing the paints without damaging the polymers. The burning of particles would potentially release more CO_2 into the environment, so an alternative to generating nanostructures without burning templates would be highly desirable [14]. For the best structural and optical properties of high-temperature CSP paint, it is necessary to develop a low-cost and highly facile method to generate reduced surface stress, solar absorbing paint coatings.

In this work, black oxide coatings in silicon matrices were developed by optimizing solvent/resin mixtures with solvents of varying evaporation rates to produce thermodynamically stable colloids. The result is a slow drying, evenly dispersed coating with reduced stress from pore-like nanostructures. With these two properties, we can develop films with porous nanostructures that have excellent mechanical and optical properties. This method does not require any additional manufacturing steps and only changes the material used to thin the pigment and resin. In addition, solvent blends can incorporate volatile organic compounds (VOCs)-exempt materials, to develop high-temperature coatings with extremely low volatile components, compared to high-temperature paints currently on the market. These changes would be significant in helping the paints comply with federal and state paint standards of USA due to an increasing desire to reduce VOCs in the paint that can degrade the environment. The purpose of this work focuses on the development of a porous CSP coating with advanced optical properties, strengthened mechanical properties, low environmental impact, and low cost of manufacturing.

EXPERIMENTAL

1. Synthesizing Induced Porous Solar Absorbing Paint and Fabrication of Solar-absorbing Tile

In preparation of solar-absorbing paint, commercially available silicon resin product Silikophen P80/X glass binder was obtained from Evonik Industries (USA). $CuCrMnO_4$ black oxide powder with bulk density of 0.9 g/mL was purchased through (Fuyang Taian Chemical Co. Ltd., China). The solvents are ACS reagent grade of xylene ≥98.5% (Sigma-Aldrich Chemical Co. Ltd., USA), anhydrous dimethyl carbonate ≥99% (DMC; Sigma-Aldrich Chemical Co. Ltd., USA), anhydrous ethylbenzene 99% (EB; Sigma-Aldrich Chemical Co. Ltd., USA) and tert-butylbenzene 99% (TBB; Sigma-Aldrich Chemical Co. Ltd., USA), anhydrous toluene 99.8% (Sigma-Aldrich Chemical Co. Ltd., USA), and isobutanol ≥99% (IBA; Sigma-Aldrich Chemical Co. Ltd., USA). For the synthesis of paint coatings, a volumetric mixture of 3 : 2.5 : 4.5 of $CuCrMnO_4$ pigment, silicon resin, and solvent mixture was placed in a glass vial filled 50% with yttrium-stabilized zirconia balls. The solid loadings on the colloid were kept constant to ensure the viscosity of the paints was approximately the same so that the spray coating process led to similar coating thicknesses between 10 and 15 μm for all the coatings. The dilution of the solids remained constant as well, the only parameters changed were the ratios of different solvents used in the mixture, which did not lead to strong changes in viscosity compared to changing the solids content. Paints were ball milled for 24 hours at 70 rpm in a rolling ball mill, and then spray coated on 1x1 square inches Haynes 230 coupons (Haynes International, USA). Samples were sintered at 150 °C for 1 hour, 250 °C for 30 minutes, 550 °C for 3 hours, and 750 °C for 2 hours with a ramping rate of 5 °C/min. For these paints, the solvent blend was changed to blends of solvents with xylene, toluene, EB, TBB, IBA, and DMC. DMC is a classified VOC exempt solvent with a faster evaporation rate than aromatic solvents [15]. Binary and ternary blends of solvents were formulated for paint VOC content less than 420 g/L and maximum incremental reactivity (MIR) values less than 1.6. Table 1 shows different binary and ternary blends of solvent used for dispersing the pigment/resins system. Samples were compared to an original sample using a 3 : 1 blend of xylene and IBA, a blend used in previous recipe coatings and used to dissolve the silicone resin [8,16].

Table 1. Chemical composition of binary and ternary solvent for porous solar absorbing paint

Binary sample blend		Ternary sample blend	
Composition	Volumetric ratio	Composition	Volumetric ratio
Xylene : IBA	3 : 1	TBB : EB : DMC	1.5 : 1.5 : 1
Xylene : DMC	2.8 : 1.7	TBB : Xylene : DMC	2.4 : 1 : 1.1
EB : DMC	3 : 1	TBB : Toluene : DMC	2.2 : 1 : 1.1
Toluene : DMC	3 : 1		
TBB : DMC	3 : 1		

2. Characterization of Solar Absorbing Tiles

FEI Apreo and Quanta (Thermo Fisher Scientific, USA) scanning electron microscopes were used to investigate the surface morphology of spray coated samples. Optical profiles were developed using a UV-3600 for UV-Vis-NIR light ranging from 220 nm and 2,600 nm and an IRTracer-100 for FT-IR radiation between 2.5 and 25 μm (Shimadzu Co., Ltd., Japan).

3. Measurement of Figure of Merit (Sunlight to Electric Power Conversion Efficiency)

To characterize the solar absorbing performance of the paints, a figure of merit (FOM) value must be calculated to weigh the solar energy being absorbed, against the thermal energy being emitted at the intended operating temperature. A formula for calculating this value is

$$\mathrm{FOM}=\frac{\int_0^{\infty}(1-\mathrm{R}(\lambda)\mathrm{I}(\lambda)\mathrm{d}\lambda-\mathrm{C}^{-1})\int_0^{\infty}(1-\mathrm{R}(\lambda)\mathrm{B}(\lambda,\mathrm{T})\mathrm{d}\lambda)}{\int_0^{\infty}\mathrm{I}(\lambda)\mathrm{d}\lambda} \quad (1)$$

where λ is the wavelength of light (nm), R(λ) is the reflectance at wavelength λ, I(λ) is the solar radiation at wavelength λ (ASTM

G173), B(λ, T) is the black body emissivity at temperature T and wavelength λ, and C is the solar concentration ratio [17]. The equation assumes the coatings are optically opaque and the spectral reflectance is independent of temperature. Therefore, the solar absorption of the coatings is independent of temperature, but the thermal radiation is not because it is taken against the black body spectrum at 800 °C. FOM values were calculated under the assumption that next generation CSP plants will operate at 800 °C and a solar concentration ratio of 1,300, and reflectance profiles were measured from 220 nm to 25,000 nm.

4. Measurement of Solar Absorbing Paint Dispersion

Measurement of the dispersion property of the resin in a solvent blend involves using the Gibbs free energy of mixing, where a negative value corresponds to a stable mixture and positive values correspond to unstable, immiscible mixtures. The Gibbs free energy (ΔG) of mixing for polymer-solvents blends can be estimated by,

$$\Delta G = \Delta H - T\Delta S \quad (2)$$

where ΔG is the Gibbs free energy of mixing [18], ΔH is the enthalpy of mixing, ΔS is the entropy of mixing, and T is the mixing temperature. The enthalpy of mixing can be calculated by the equation,

$$\Delta H = kTN\chi_{sol}\chi_{res}\chi \quad (3)$$

where k is the Stefan Boltzmann constant, T is the temperature of mixing, N is the total number of molecular lattice sites in solution, χ_{res} is the molecular fraction of the resin segments in solution, χ_{sol} is the molecular fraction of solvent molecules in solution, and χ is the Flory Huggins interaction parameter calculated with the Hildebrand solubility parameters plus an entropic contribution [18-21]. The lattice theory for mixing states that a solution makes up a lattice matrix and each unit in the lattice can be occupied by either a solvent molecule or a segment in the resin chain [18]. The enthalpy of mixing measures the thermodynamic stability between the polymer chains and the solvent. The entropy of mixing could be approximated by,

$$\Delta S = NK\left[\frac{\chi_{res}}{n}\ln(\chi_{res}) + \chi_{sol}\ln(\chi_{sol})\right] \quad (4)$$

where n is the number of segments in the polymer chain. In lattice theory the change in entropy is a measure of the number of possible combinations the solvent and resin can occupy on individual lattice in a matrix [22]. Both the enthalpy and entropy terms were multiplied by the number of lattice sites to achieve the Gibbs free energy of the resin-solvent matrix, not just a single lattice site. The results of the previous study vary between using volume or mole fractions depending on their experiments [23], but molecular (molar) fractions were used in this experiment for its better representation of the qualitative data.

5. Measurement of the Environmental Impact of Solar Absorber Coatings

An important characteristic to account for when synthesizing paint is its environmental footprint. This study uses two different methodologies to measure the effects of the paint on the environment. The first is the VOC content of the paint, which measures the mass of volatile components of a solution to the total volume of the solution minus any VOC-exempt parts [24]. The second method of measuring the environmental impact of the paint coating is the MIR value. An incremental reactivity value is a measure of the photocatalytic activity of an individual solvent species (amount of ozone produced per VOC emitted). The maximum incremental reactivity weighs the individual incremental relativities by their weight percentages and sums each component in the coating [24]. Unlike the VOC content, which measures the amount of volatile component in a paint, the MIR measures how volatile and harmful the solvent blends in coatings are to the environment.

RESULTS AND DISCUSSION

1. Gibbs Free Energy of Mixing

Spinel black oxide nanoparticles suspended in organic media using steric stabilization from an-adsorbed polymer resin. The Si-O and O-H bonds along the backbone and tail of the poly (methyl phenyl siloxane) bond to the surface of the $CuCrMnO_4$ particles through dipole forces, protruding the methyl and phenyl-functional groups into solution. The particles with the adsorbed polymer are then thermodynamically stabilized using steric stabilization principles. One of the factors of dispersion and stabilization of the particles is the choice of solvent [25]. Optimizing the blend of solvents with the best interactions with the phenyl and methyl groups will allow more control over the surface structure [26]. To measure the effectiveness of the solvent on mixing with the polymer, Gibbs free energy values were calculated. Mixtures with strongly negative Gibbs free energy values will have thermodynamically stable mixing properties, meaning the resin and solvent mixture are homogeneous and the solid and liquid portions will not separate as quickly. Weakly negative Gibbs free energy values will have much weaker dispersion properties of the silicone polymer resin, leading to clumping of the resin and pigments, which can lead to a poor surface structure during the coating process. [18].

To calculate the Gibbs free energy of mixing, the enthalpy, and entropy of mixing values each had to be calculated. For a poly (methyl-phenyl-siloxane) resin the solubility and molar volume (per segment) were taken to be 18.41 $Mpa^{0.5}$ and 106 cm^3/mol from previ-

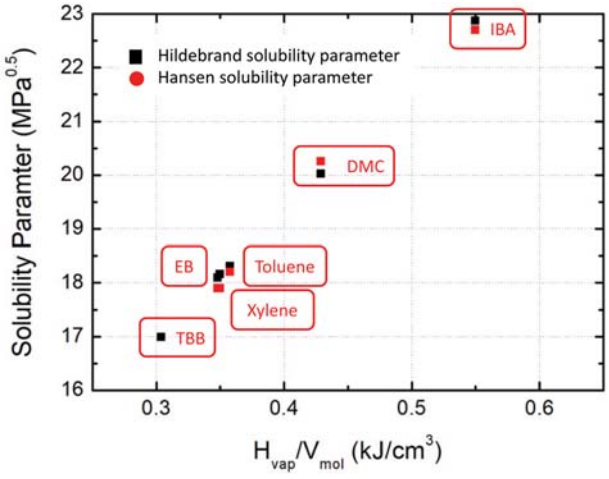

Fig. 1. Hildebrand solubility parameter as a function of heat of evaporation over molar volume.

Table 2. Gibbs free energy values for various solvent blends in porous solar absorbing paint

Solvent blend		Interaction parameter	ΔH (J/mol)	TΔS (J/mol)	ΔG (J/mol)
Binary solvent	Xylene/IBA	1.54	466	375	90
	DMC	2.97	955	391	564
	DMC/Xylene	1.37	429	384	44
	Toluene/DMC	0.56	175	382	−207
	EB/DMC	0.45	137	377	−240
	TBB/DMC	0.49	144	368	−225
Ternary solvent	TBB/EB/DMC	0.34	102	373	−271
	TBB/Xylene/DMC	0.37	110	371	−261
	TBB/Toluene/DMC	0.36	108	373	−265

ous study [27,28]. The molecular weight of the specific Silikophen resin used was only provided in a range, so the larger size of the molecular weight (3,000 g/mol) was used as a more stringent test for solubility [29]. Using molar volume and heat of evaporation attained from [30,31], the Hildebrand solubility parameters were calculated and can be seen in Fig. 1. Note that Hildebrand solubility parameters are not highly accurate for polar solvents because they do not contribute any factors for dipole interactions or hydrogen bonding [21], but since the two values have less than a 1.5% difference and most the solvents used are nonpolar Hildebrand is an acceptable simplification. With the solubility parameters calculated, the Flory-Huggins interaction parameter was calculated to test the enthalpic favorability of the silicone polymer in the different blends of organic solvents. Samples with solvent blends of DMC and xylene, DMC, and xylene and IBA have much larger interaction parameters (>1) than the other samples. All calculated interaction parameters, enthalpies of mixing, entropies of mixing, and Gibbs free energies of mixing can be found in Table 2. Out of all the samples only the xylene/IBA, DMC, and xylene/DMC displayed unfavorable solvent/resin compatibility due to the positive Gibbs free energy of mixing values.

2. Surface Morphology of Paint Coatings with Binary and Ternary Solvent Blends

Solvent evaporation rate also plays a critical role in film formation of paint coatings. For each sample, the evaporation rate was calculated using the solvent's vapor pressure [32], whose values were obtained from the previous study [33] and then normalized to the solvent with the slowest evaporation rate (TBB). The evaporation rates of all the solvents plus some of their environmental properties can be seen in Table 3. By blending solvents with negative Gibbs free energy values and different evaporation rates we can control the surface structure of the coating. Previous literature used xylene and IBA because the phenyl and hydroxide functional groups were thought to stabilize the siloxane resin. However, Gibbs Free Energy calculations show that blending using the given ratios of the solvents yields poor dispersions. SEM images in Fig. 2(a) show over 50 μm cracks propagating due to stresses in the film from poor dispersion of the nanopowders and rapid drying after the sintering process [26,34]. More enhanced SEM imaging in Fig. 2(b) shows the formation of pigment/resin agglomerates up to 1-2 microns in size due to the solvent/resin separation in solution. Particle agglomeration and micro-cracking will decrease the long-term optical and mechanical properties of the applied coating. As the

Table 3. Environmental and physical properties of different organic solvent for porous solar absorbing paint

Solvent	MIR value	VOC status	Vapor pressure (mmHg)	Evaporation rate (relative to TBB)
DMC	0.06	Exempt	55.4	27
Toluene	4	VOC	28.4	14
EB	3.04	VOC	9.6	4.5
Xylene	7.64	VOC	8.8	4.1
TBB	1.95	VOC	2.2	1
IBA	5.25	VOC	10.4	4.9

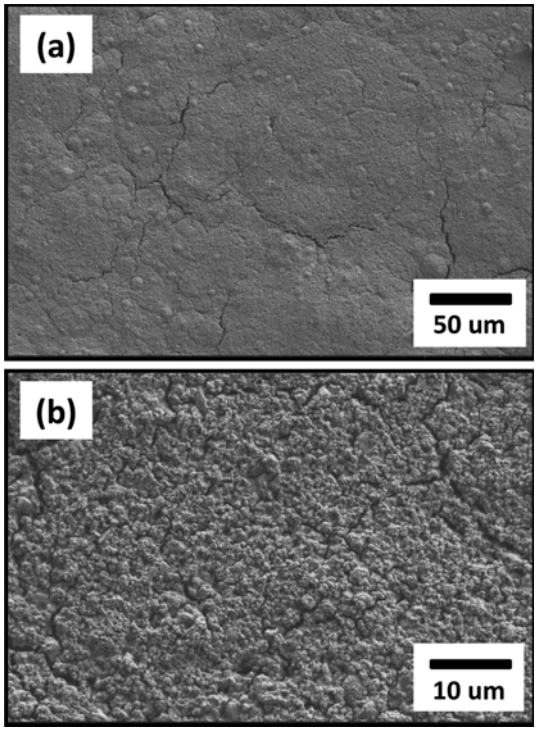

Fig. 2. SEM surface images of typical CSP receiver coating layer prepared with xylene/IBA blend: (a) Close up image; (b) zoomed out image.

nanoparticles agglomerate their optical absorbance decreases, decreasing their optical performance, and their overall performance as a solar absorber coating. Also, if the micro-cracking continues to propagate and expand due to thermal cycling and long-term temperature exposure at 800 °C, the films can begin to peel off the Haynes alloy tubing. Both the optical and mechanical issues would require premature re-application of the coating.

Binary blends of solvent were then tested using 3 : 1 blend of aromatic solvent to DMC. DMC was used for its quick evaporation rate and VOC exempt status, but alone DMC has very low affinity for the silicone resin, as seen by the difference in solubility parameters. Early attempts to develop paints with higher ratios of DMC resulted in destroyed films as seen in Fig. 3. These colloids have unstable thermodynamic mixing according to Gibbs free energy values, but unlike the xylene/IBA mixture, the DMC mixtures have higher evaporation rates, leading to a highly stressed film which peeled off the substrate. TBB, EB, and toluene were also selected as aromatic hydrocarbons. Xylene is a common solvent used in paint but was not chosen because the goal MIR value below 1.6 could not be achieved with a 3 : 1 ratio of xylene and DMC due to xylene's high MIR value. Fig. 4 shows the surface structure of all the binary solvent blends. The degree of cracking in coating samples decreases from toluene to EB to TBB due to the decreasing evaporation rates of the aromatic solvents. The cracks for the toluene and EB blends decrease to below 50 μm, while the TBB blend exhibits little to no crack propagation on the surface. All the painted blend samples have negative Gibbs free energy values, meaning the resin has favorable solubility with the binary blend. Enhanced dispersion and slow evaporation rates improve the film qualities by reducing surface stress due to shrinkage and particle aggregation.

Unlike the samples that use toluene and EB, which dry into a high nanoparticle dense surface, the mixture of DMC and TBB demonstrates a more dispersed nanoparticle film, leaving behind pinhole-like pores on the surface. This result is due to the thermodynamically stable resin-solvent interaction and the use of a slower evaporation solvent (TBB). The colloid is well dispersed upon application of the paint unto the substrate, meaning the coated nanoparticle/resin matrix is also well dispersed on the substrate. Then the use of a slowly evaporating solvent relieves stresses evenly throughout the sample, leaving behind pinhole-like pores as points of stress relief instead of microcracking across the surface. Ternary blends using DMC, TBB, and a third aromatic component were also tested to generate a stress-free surface.

Fig. 5 shows the SEM surface images for samples thinned with

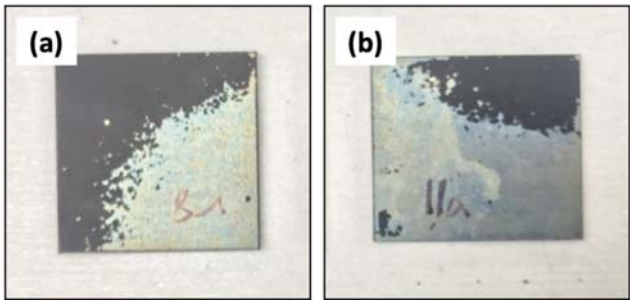

Fig. 3. Photograph of porous CSP receiver coating layer prepared with (a) DMC and diluted with a (b) DMC/xylene blend.

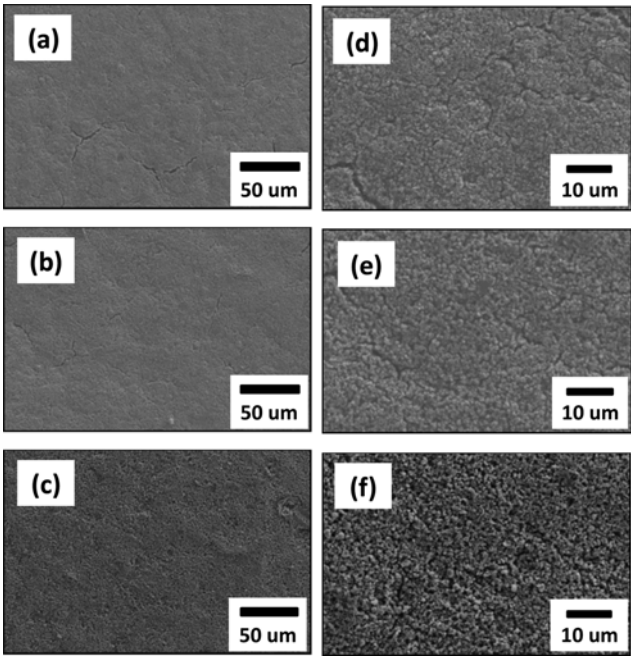

Fig. 4. SEM surface images of porous CSP receiver coating layer prepared with binary solvent such as (a), (d) toluene/DMC blend, (b), (e) EB/DMC blend, and (c), (f) TBB/DMC Blend (a)-(c): Low magnitude, (d)-(f): High magnitude).

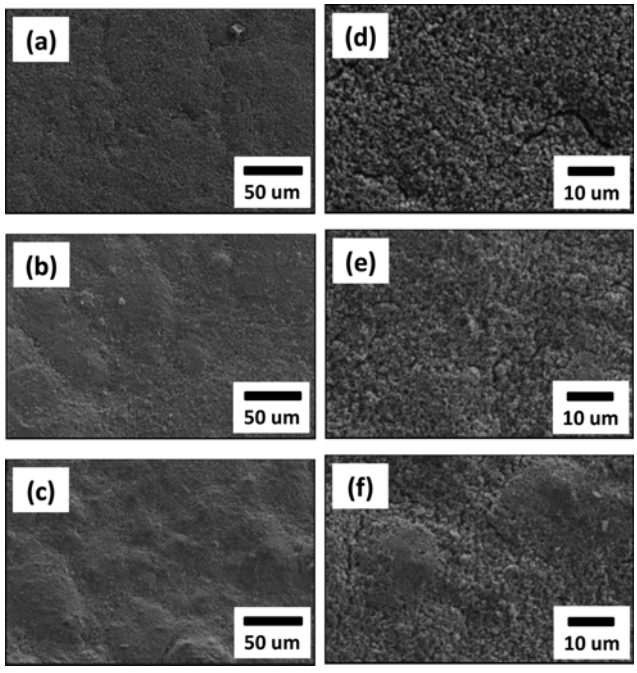

Fig. 5. SEM surface images of porous CSP receiver coating layer prepared with ternary solvent such as (a), (d) TBB/EB/DMC blend, (b), (e) TBB/xylene/DMC blend, and (c), (f) TBB/toluene/DMC ((a)-(c): Low magnitude, (d)-(f): High magnitude).

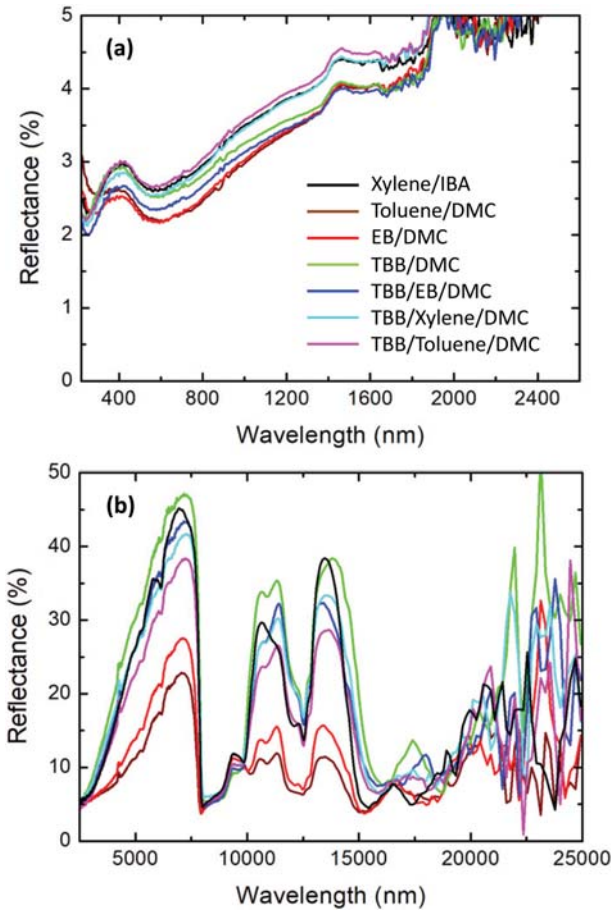

Fig. 6. Vis/NIR/IR optical profiles of porous CSP receiver coating layer prepared with different solvent composition.

ternary blends of solvents. The first attempt used an equal volume ratio of TBB and EB, which led to the same phenomena of porous surface release like with the binary blend of TBB and DMC. Even though surface pores were created, the film still suffered some micro-cracking due to the elevated evaporation rate of EB in comparison to TBB. The next two samples used a 2.4 : 1 : 1.1 ratio of TBB to xylene/toluene to DMC. These samples have patches of porous zones and densely packed zones, attributed to phase separation between the solvents in the paint colloid. The different blending of solvents can affect the structure of the applied coating which can in turn affect the optical properties of the paint as well.

3. Optical Properties of Solar Absorber Coatings

In addition to examining the surface structure of the paints, optical data was obtained to evaluate the coating's capabilities as a solar absorber. Fig. 6 shows the optical profile of the different CSP coatings and Table 4 shows the solar absorbance, thermal emittance, and FOM of each sample. The optical profile in the UV-VIS-NIR range remains similar for all the coatings, with a maximum difference of about 0.5% between the DMC/toluene/TBB blended paint and the DMC/EB blended paint as seen by the values in Table 4. The FT-IR profile, however, remains vastly different for all samples, with emissivity differences between the maximum and minimum samples of nearly 10%. Lower emissive samples probably stem from the thickness of the coating, where thinner samples exhibit a higher degree of reflection from the back surface of the Haynes 230 alloy. Pore-like structure in the coatings could help to scatter incident solar radiation, allowing the coatings to achieve higher solar absorbances at thinner thicknesses. However, weaker solar-absorbing materials would be needed to test the effects of pore-structure on light scattering. Weaker solar absorbance is necessary because the solar absorbance of the current black oxide coatings is so high that any changes in structure would show insignificant change on the optical properties of the coating. While all paints exhibit strong solar to thermal conversion performance, the ones with the enhanced micro-structure from effective solvent blending had the highest FOM values of 0.9160 for the TBB/DMC blend and 0.9163 for the TBB/EB/DMC blend, a 0.3% increase from the original reference blend, which can be attributed to the enhanced microstructure of the coating. The change may seem small but is significant considering we are approaching the maximum theoretical figure of merit at the given operating parameters. With the increase in efficiency, more energy can be absorbed without radiating back into the environment, which can be conducted into the heat transfer media, and converted into useable energy generated by the CSP plant. This low increase can significantly increase the energy generated by the plant which can decrease the levelized cost of electricity of CSP power tower plants.

4. Environmental Properties of Solar Absorber Coatings

To minimize the environmental footprint of the paint, all samples were synthesized using solvent blends that lower the VOC content value below 400 g/L. The calculated VOC and MIR values of porous CSP paint coatings with different solvent blends are summarized in Table 5. Other than the original sample with blended

Table 4. Optical properties of CSP receiver coating layers prepared with various solvent compositions in porous solar absorbing paint

Sample index		FOM	Absorbance	Emissivity
Binary solvent	Xylene/IBA ([a]reference)	0.9134	0.9675	0.8429
	Toluene/DMC	0.9133	0.9720	0.9134
	EB/DMC	0.9140	0.9719	0.9014
	TBB/DMC	0.9160	0.9686	0.8193
Ternary solvent	TBB/EB/DMC	0.9163	0.9704	0.8422
	TBB/Xylene/DMC	0.9137	0.9676	0.8388
	TBB/Toluene/DMC	0.9116	0.9667	0.8579

[a]Reference is based on prior resin dilution

Table 5. Environmental properties of porous CSP paint coatings with different solvent blends

Sample index		Environmental properties	
		VOC content (g/L)	MIR
Binary solvent	Xylene/IBA ([a]reference)	441	3.32
	Toluene/DMC	395	1.58
	EB/DMC	395	1.39
	TBB/DMC	395	1.04
Ternary solvent	TBB/EB/DMC	395	1.21
	TBB/Xylene/DMC	395	1.58
	TBB/Toluene/DMC	395	1.38

[a]Reference is based on prior resin dilution

xylene and IBA, all samples meet this criterion and the criteria in most counties in California of a maximum VOC content of 420 g/L for high-temperature coatings [37]. If the paint can meet California VOC standard, which are some of the strictest environmental standards in the country, it can provide a good global standard for paints with reduced environmental impacts. These values are also lower than the industrial standard Pyromark 2500 with VOC content of 695 g/L [38]. High-temperature coatings have a much less stringent requirement than flat paints because of the high-temperature silicone resins. Most of the resins that exist to handle the operation of high-temperature CSP have little to no miscibility in water and require organic media for suspension. Most of the paints require the use of organic solvents and, therefore, the VOC content requirement of these paints is more acceptable [29,39].

The MIR values of each coating have more variation because of the stronger effects of each individual component on the MIR value. The reference sample has a large MIR value (3.22) because of the abundance of xylene in solution, which has an MIR of 7.64 [40]. Because of the abundance of organic solvents, Pyromark 2500 also has a high MIR value between 2.25 and 3.15 [40]. Substituting xylene with toluene (4), EB (3.04), or TBB (1.95), and IBA with DMC (0.06) reduces the MIR significantly due to their smaller incremental reactivity values. Specifically, the usage of TBB can bring the MIR value down to 1.04, much lower than the California standard of 1.85 [41] for high-temperature coatings because TBB has a lower degree of reactivity with its environment than other solvents, meaning it will release less ozone [42]. As with the VOC content, if the paint can meet California's more strict MIR standards, it could provide strong global trends for reducing the environmentally degrading components of paints. Adoption of solvent blends like this goes far in creating more environmentally compatible paints that can promote the generation of solar energy and reduce atmospheric pollution from volatile compounds.

5. Economics of Solar Absorber Coatings

Naturally inducing pores through solvent selection is the most economical method of synthesizing large-scale porous CPS paint. Current CSP paint processing uses ball milling to disperse black oxide powders, silicon resins, and thinning solvents. Usage of sacrificial polymers such as polystyrene would add extra steps to the manufacturing because the sacrificial polymers would be destroyed during the milling process; therefore, a post-processing step is required to ultrasonically distribute sacrificial polymers into the colloid mixtures. Capital equipment for the ultrasonic dispersion could cost upward of $25,000 and would also increase labor costs (Shanghai ELE Mechanical and Electrical Equipment Co., Ltd., China). Optimizing the solvent blend would not add any additional steps to the process, because the wetted pigment has to be thinned with the solvent eventually, the optimized mix can just be added in at this step in the manufacturing process. Material cost of the custom sized sacrificial polymers is too high for commercialization (~$150/kg of customized size polymer beads, Esprix Technology, Inc, USA), in comparison to the relatively low costs of solvents (<$10/kg, ChemFine International Co., Ltd., China). Altogether, porous CSP paints synthesized using polystyrene beads could cost greater than $250/L, while using solvents would reduce the cost to ~$100/L, cost competitive to the industry standard Pyromark 2500 CSP paint. The improved structure from the solvent blending could also significantly increase the lifetime of the paints on the receivers, making an effective, low-cost alternative to traditional CSP paints.

CONCLUSION

Naturally, porous CSP paints could be synthesized by optimizing a solvent blend with thermodynamically stable solvent/resin mixtures and slow evaporating solvents. Using a blend of TBB and DMC, a coating with natural porosity, virtually no surface cracking, and strong optical performance (FOM of 91.6%) was synthesized. Utilization of these solvents also helps reduce the paint's environmental impact, specifically by reducing the VOC content and MIR value to 395 g/L and 1.04, respectively. Using a solvent blend with slow evaporation rates and favorable thermodynamic colloid stability, we were able to create a CSP paint coating with enhanced optical properties, high mechanical strength, lower environmental impact, and incredibly low cost.

ACKNOWLEDGEMENTS

This research is funded by the Department of Energy Sunshot-Apollo project (DE-EE0007113). The authors are grateful to Solar Reserve, LLC for helpful discussions.

REFERENCES

1. J. Nelson, The Physics of Solar Cells. Imperial College Press, London, UK (2003).
2. M. Gratzel, *Nature*, **414**, 338 (2001).
3. H. L. Zhang, J. Baeyens, J. Degreve and G. Caceres, *Renew. Sust. Energy Rev.*, **22**, 466 (2013).
4. D. Barlev, R. Vidu and P. Stroeve, *Sol. Energy Mater. Sol. Cells*, **95**, 2703 (2011).
5. A. Green, C. Diep, R. Dunn and J. Dent, *Energy Procedia*, **69**, 2049 (2015).
6. A. Boubalt, C. Ho, A. Hall, N. Lambert and A. Ambrosini, *Renew. Energy*, **85**, 472 (2016).

7. C. K. Ho, A. Mahoney, A. Ambrosini, M. Bencomo, A. Hall and T. N. Lambert, *ASME. J. Sol. Energy Eng.*, **136**, 14502-014502-4 (2013).
8. T. Kim, B. VanSaders, J. Moon, T. Kim, C. Liu, J. Khamwannah, D. Chun, D. Choiu, A. Kargar, R. Chen, Z. Liu and S. Jin, *Nano Energy*, **11**, 247 (2015).
9. Q. Geng, X. Zhao, X. Gao, H. Yu, S. Yang and L. Gang, *Sol. Energy Mater. Sol. Cells*, **105**, 293 (2012).
10. R. Bayón, *Renew. Energy*, **33**, 348 (2008).
11. J. Vince, *Sol. Energy Mater. Sol. Cells*, **79**, 313 (2003).
12. C. E. Kennedy, Review of Mid- to High-Temperature Solar Selective Absorber Materials. TP-520-31267, NREL: Lakewood, CO (2002).
13. R. C. Pohanka, R. W. Rice and B. E. Walker, *J. Am. Ceram. Soc.*, **59**, 71 (1976).
14. Z. Wang, J. Wang, H. Richter, J. Howard, J. Carlson and Y. Levendis, *Energy Fuels*, **17**, 999 (2003).
15. I. Francesco, B. Cacciuttolo, M. Pucheault and S. Antoniotti, *Green Chem.*, **17**, 837 (2015).
16. Silikophen P80/X: Technical Datasheet. Evonik, Essen, Germany, October (2016).
17. J. Moon, T. K. Kim, B. VanSaders, C. Choi, Z. Liu, S. Jin and R. Chen, *Sol. Energy Mater. Sol. Cells*, **134**, 417 (2015).
18. J. S. Higgins, J. E. G. Lipson and R. P. White, *Phil. Trans. R. Soc. A*, **368**, 1009 (2010).
19. A. Marciniak, *Int. J. Mol. Sci.*, **11**, 1973 (2010).
20. A. J. Marzocca, A. L. Rodríguez Garraza and M. A. Mansilla, *Polym. Test.*, **29**, 119 (2010).
21. M. Belmares, M. Blanco, A. Goddard, R. B. Ross, G. Caldwell, S. H. Chou, J. Pham, P. M. Olofson and C. Thomas, *J. Comput. Chem.*, **25**, 1814 (2004).
22. N. Young, Thermodynamics and Phase Behavior of Miscible Polymer Blends in the Presence of Supercritical Carbon Dioxide. Ph.D. Dissertation, University of California Berkeley, Berkeley, CA, USA (2014).
23. L. Robeson, Polymer Blends: a Comprehensive Review, Hanser, Cinncinati, USA (2007).
24. R. Litton, Challenges and solutions Solvent technology for present and future air quality regulations. Eastman Chemical Company, Kingsport, TN, USA (2013).
25. J. Shi, Steric Stabilization. Center for Industrial Sensors and Measurements, Ohio State University: Columbus, Ohio, USA (2002).
26. R. Anderson, "Stress Free Coatings Made Possible by Solvents Eastman Chemical Company, Kingsport, TN, USA (2004).
27. Polymer Database (2017) Names and Identifiers of Polymer. http://polymerdatabase.com/polymers/Polymethylphenylsiloxane.html (accessed 3/7/2018).
28. G. Floudas, M. Paluch, A. Grzybowski and K. L. Ngai, Molecular Dynamics of Glass Forming Systems. Springer, New York, USA (2011).
29. Technical Background Silicon Resins. Evonik, Essen, Germany (2014).
30. United States Environmental Protection Agency (Chemistry Dashboard), https://comptox.epa.gov/dashboard (accessed Mar 14, 2018).
31. J. Chickos and W. Acree, *J. Phys. Chem.*, **32**, 1880 (2013).
32. D. Mackay and I. Wessenback, *Environ. Sci. Techno.*, **48**, 10259-63 (2014).
33. Pubchem, https://pubchem.ncbi.nlm.nih.gov (accessed Mar 14, 2018).
34. R. Ashiri, A. Nemati and S. Ghamsari, *Ceram. Int.*, **40**, 8613 (2014).
35. M. Debral, J. F. Francis and L. E. Scriven, *AIChE J.*, **48**, 25 (2002).
36. K. Katsogiannis, G. Vladisavljevic and S. Georgiadou, *Eur. Polym. J.*, **69**, 284 (2015).
37. California Air Resources Board, https://www.arb.ca.gov/coatings/arch/rules/VOClimits.pdf (accessed Mar 14, 2018).
38. Pyromark High Temperature Paint 2500 Flat Black (MSDS No. LACO1508007), LA-CO Industries, Elk Grove Village, IL, USA (2012).
39. R. Joesph, *Metal Finishing*, **108**, 78 (2010).
40. California Air Resources Board, https://www.arb.ca.gov/consprod/regs/2015/mir_tables_final_ 1-22-15.pdf (accessed Mar 14, 2018).
41. California Air Resources Board, https://www.arb.ca.gov/consprod/regs/2015/article_3_final_1-22-15.pdf (accessed Mar 14, 2018).
42. W. Carter, J. Pierce, D. Luo and I. Malkina, *Atmos. Environ.*, **29**, 2499 (1995).